Development of a small-scale actuator disk

Author
SANNE DE JONG HELVIG

Supervisor
R. JASON HEARST

December 6, 2019

NTNU – Trondheim
Norwegian University of
Science and Technology

Table of Contents

Figures

Abstract

In this thesis, the drag of a small-scale rotating wind turbine model is measured in a wind tunnel. Actuator disks, with three different solidities and two different layouts, were designed and 3D printed. Then, the drag on the ADs was measured, and the results compared to the rotating wind turbine models in order to find the best match. The disk with a non-uniform design and a solidity of 35% turned out to be the closest match.

Acknowledgements

I would first and foremost like to thank my supervisor Jason Hearst, for always helping me out and supporting me, and for arousing my interest in aerodynamics in the first place. Through weekly meetings he has continued to push me and give me helpful input every step of the way, and he was always available when I needed som additional guidance.

I would also like to thank Magnus Kyrkjebø Vinnes, for helping me out whenever I got stuck and for his patience and positivity whenever we were troubleshooting. My thesis would not be what it is without your guidance.

I want to thank Lars Morten Bardal, for teaching me how to do calibrations, how to use the wind tunnel and for making the LabView program that he so kindly let me use.

I also want to give my thanks to Olav Rømcke, for teaching me how to use power tools, and the rest of Jason's Ph.D. students for all their helpful input at out weekly meetings.

Finally, I want to thank Adrian Bogen Skibelid, for proof reading, for all our sessions of throwing ideas back and forth, and for your continuous support.

Chapter 1

Introduction

In a world with a growing population, growing standards of living, and with it, a growing need for energy, simultaneous with an increasing focus on sustainability and environmentally friendly solutions, renewable energy has never been more relevant. The amount of onshore and offshore wind power is increasing, and numerous companies are working to find their role in the new market. Optimizing wind turbines and wind farms is an important aim, and researchers are using both simulations and experimental methods in order to explore different potentially efficient solutions.

However, within both methods, modeling a wind farm with moving blades is often extremely complicated. Thus, simplifications, such as the actuator disk, are commonly adopted. The idea of the actuator disk is that it produces the same drag as the wind turbine, resulting in similar bulk characteristics in the wake. The physical wind tunnel analogue to an actuator disk is a static, porous disk. However, at this point in time, there are no clear directions and no scientific consensus on how to design and make these porous disks in order to mimic rotating turbines when conducting experiments.

1.1 Problem formulation

The objective of the project described in this thesis is to develop a static, porous disk that has approximately matched characteristics to a small rotating wind turbine model provided by KTH, by matching the produced drag. In order to achieve this, the drag of the rotating wind turbine models are measured, and a variety of small-scale actuator disks are designed and 3D printed before drag measurements of the disks are conducted. Based on the results, the design will be honed in order to match the drag as closely as possible.

Chapter 2

Background

Within the field of wind turbine aerodynamics, the actuator disk theory describes the simplest way to model a rotating turbine. The actuator disk is a non-rotating disk, physically modeled as a static porous disk. The idea is that the actuator disk produces the same drag as a moving turbine, resulting in the same bulk characteristics in the wake.

The drag on the wind turbine models is the force in the direction parallel to the direction of the wind. The drag coefficient is further defined as

$$C_d = \frac{D}{\frac{1}{2} * \rho * u^2 * A} \tag{2.1}$$

where ρ is density, u is the flow velocity and A is the reference area.

The drag on an object changes as the velocity changes. According to theory, C_d increases as Re increases and then C_d levels of at $Re \simeq 10^3$, after which it remains approximately constant within the boundary of laminar flow. So this is the typical profile to expect when conducting drag measurements with varying Re. Here, Reynolds number is defined as

$$Re = \frac{\rho * u * L}{\mu} \tag{2.2}$$

where ρ is density, u is velocity, L is characteristic length and μ is the dynamic viscosity. For Reynolds number lower than $\simeq 5 * 10^5$ the flow is laminar, which is the type of flow relevant for this project.

The porosity is a measure of the permeable area of the disc and is defines as the ratio between the open area and the total area of the disc.

The renewed interest in wind energy originated in part from large funding programs by the American and European governments and from the realization that wind energy will be

a important contributor to production of affordable and clean energy in the next decades. A contribution to the overall electricity production of up to 20% is aimed by 2030, but to realize these targets, larger wind farms covering increasingly larger surface areas are required [12]. They wind turbines will grow not only in size, but also in capacity and money invested [3].

Current utility-scale turbines extend a significant distance into the atmospheric boundary layer, which is naturally turbulent [14] [11]. Further, placing the turbines in wind farms is the most economic and and efficient when it comes to planning, use of land and infrastructure, and maintenance [14]. Thus, wind turbines are permanently exposed to turbulence, either within the wind or when downstream turbines are hit by the turbulent wake created by upstream rows of turbines and their rotating turbine blades [14] [11].

Within a wind farm, as kinetic energy has been extracted from the wind and converted into electricity, the wind speeds do not recover to their freestream value after encountering the first row of turbines, and thus the wind speeds hitting subsequent turbines are lower than the freestream value [3]. Thus, the wake from the upstream wind turbines determine how much power a downstream turbine can generate and which mechanical loads it experiences, meaning that the study and characterization of wind turbine wakes has become an important research area. [14] [11] When turbine spacing and wind farm layouts are considered in a conventional approach, decisions are made based on the desire to limit the wake-induced fatigue loads on downstream turbines [12].

Variability in power output from wind turbines due to unsteady characteristics of the ABL is a challenge for the integration of large amounts of wind energy into the electricity grid, and the need for fill-in power and stronger components made to withstand unsteady loading turns the problem into that of a cost-minimizing problem, in order for wind energy to achieve the desired market share [5]

Studies of the interaction of large wind farms and the ABL, and how the wake develops and interacts with downstream WT arrays, are currently not prevalent, and improved knowledge and understanding of the interaction is necessary [12] [5] [16] [11] [1]. With improved understanding of this type of flows, wind farm developers can plan better-performing, less maintenance-intensive and longer-lasting wind farms, and manufacturers could create better fatigue load-mitigating designs [11].

Field tests are being carried out, but such approaches are expensive, difficult and by their nature incapable of being completely controlled [16]. Wind tunnel measurements have the advantage over full-scale experiments that the inflow and boundary conditions can be carefully controlled, and thus they can bring additional insight. [5]. Additionally, a wide range of inflow conditions can be tested and the created wake can be studied [16]. However, it should be mentioned that there is a need for increased amounts of data from actual wind farms, to evaluate whether experimental results are representative for the actual case.

A challenge for studying wind farms in wind tunnels is performing measurements with sufficiently high temporal and spatial resolution for a turbine array containing a large number of model turbines [5]. Therefore, small-scale turbines are relevant for experiments, and allow for extensive flow mapping studies to be conducted without the requirement of con-

structing scale turbines or the cost associated with large experimental test facilities[7]. The experts workshop organized by ForWind-Uni Oldenburg in 2018 on Wind Energy Science & Wind Tunnel Experiments agreed to qualify the smallest wind turbine models, with a rotor diameter less than 0.5 m, as wake-generating turbine models, independent on whether they are steady or rotating models [1].

However, using rotating blades for such small rotors, and building and operating 100 of them in a wind tunnel is not practical, but rather complex and costly. In addition, scaled rotating wind turbine models have inherent limitations since perfect flow similarity is not possible due to large scale differences. [5]. Rotating wind turbines can be compared to porous media due to their significant amount of flow-through. The question remains whether and to what extend it is possible to use simplified, non-rotating turbine models [14].

In order to study the wake, several numerical and physical modeling approaches are used. Some model the wind turbine with the simplest model, the AD concept, adding a drag source within the surface swept by the blades [2]. Porous disks are momentum sinks that does not directly extract energy from the flow, but instead dissipated kinetic energy of the incoming wind by generating small-scale turbulence in the near wake of the disk [10]. The simple but efficient actuator disk may be used as a simple method for simulating horizontal axis turbines.

Multiple experimental studies concerning ADs have already been conducted. Some are at the stage of developing the AD itself.

For example, Pierella and Sætran (2010) [15] studied the flow behind two circular grids of equal diameter and porosity but different mesh geometry. They used a biplane mesh, which turned out to produce a non-axisymmetric wake, and a monoplane mesh, giving an axisymmetric wake. The two wakes had different characteristics and the disks had different drags.

Earlier this year, nine research teams organized a round-robin measurement campaign of the wake of two porous discs in a homogeneous and low turbulent flow, performing similar wake measurements in different wind tunnels. [1] In general, results collapsed reasonably well across facilities.

Researchers such as Cannon et al. (1993) [6] have studied the wakes behind porous disks of varying solidity.

Others have gone further, and are moving towards the stage of using the actuator disks as simplifications for wind turbine models.

Bossuyt et al (2016) [5] used 100 porous disk models to model a wind farm in a wind tunnel at different layouts, in order to study power output variability and unsteady loading in a turbulent boundary layer.

Also [13] did analysis on the flow field around horizontal axis tidal turbines using mesh disks as rotor simulators.

In 1981, Sforza et al [16] used porous disks to simulate the effect of a wind turbine in

order to investigate the wake, using both experimental and numerical methods.

[14] investigated and compared an actuator disc and a model wind turbine exposed ti differnt uniform turbulent inflows, investigating the most variables. In the far wake, the wakes of both are similar. The results are independent on the inflow conditions. Velocity and turbulence intensity was different in the near wake.

A first requirement for a scaled wind turbine representation is a correct characterization of the wake structure (Theunisen et al 2015). When creating an AD to represent a WT, the starting point is often to match the diameter and the drag.

Studies conducted so far has a general agreement on the following terms. The near wake differs between the two models, as the turbulence in terms of the AD is produced by a grid, while rotating turbines introduce rotational momentum, tip and hub vorticies and turbulence from the blades (Zhang 2012). The difference in flow behaviour close to the model, especially prominent in terms of velocity deficit and turbulence intensity, is thus caused by fundamentally different turbulence production and mixing mechanisms, and leads to improper reproduction of the near flow [1].

However, blade signatures and rotational momentum have shown to be overshadowed by ambient velocity fluctuations in the far wake [2]. Porous disc models can create similar far wake as rotating models, making AD an adequate and appropriate substitution both at low and high inflow turbulence, typically from x/D = 3-4 [14] [1] [2] [9] [**?**] [**?**]. and thus the disks are acceptable when studying wake interactions at wind farm scale. Bossuyt et al 2016 concluded that the experimental setup of a model wind farm is able to capture the main trends in mean row power and unsteady loading, making it useful for layout optimization studies.

Studies have found that the drag coefficient is only weakly dependent on Reynolds number, so it remains roughly constant for a range of wind tunnel velocities. However, there is a dependence, meaning predictions of drag force with low levels of turbulence may differ from drag force experienced when operating in highly turbulent flow [4].

2.0.1 Experimentally

Lignarolo et al 2016 [10] provided an experimental analysis of the near-wake turbulent flow of a wind turbine and a porous disc. finding similarities and differences. They concluded that even in the absence of turbulence, the results show a good match in many variables such as thrust and energy coefficient, velocity, pressure and enthalpi. However, the turbulence intensity and turbulent mixing varied. The results suggested the possibility to extend the use of AD in numerical simulations until the very near wake, provided that turbulent mixing is correctly represented. The underlying question is how much the near wake differs given similarity of dimension, axial force and extracted energy. The stronger fluctuations in the WT wake are due to the pressence of concentrated tip vortices. They found the turbulence intensity of WT to be 2-4 times larger than for the AD wake in the near wake. Physics governing the turbulent mixing in the two wakes are intrinsically different. even in the absence of inflow turbulence, the velocity fields in the wakes are very

well comparable. Again, extend the use of AD in numerical simulations until the very near wake.

[10] also compared earlier experiments, showind a consistent decreasing drag coefficient with increasing porosity.

Also the other Lignarolo: [9] conducted an experiemtnal study focusing on the comparison between the wake of a turbine and an AD. WT wake caracterized by complex dynamics of tip vortex development and breakdown, and turbulent fluctuations. Wake of AD is instead characterized by isotropic random fluctuations. Looking into the limitations.

It is know that AD misestimates the effects of flow turbulence, due to the absence of the blade flow and its tip-vortes development and breakdown (Barthelie 2007). The mixing process across the wake interface and ultimately the rate at which the wake recovers the flow momentum is incorrectly modelled.

The far wake region is typically less affected by the presence of the rotating blades.

Despite the popularity of the simplified numerical model, few experimental studies are available., which analyse the flow field in he wake of an AD [9]. Matching the diameter and thrust coeff, the two give rise to the same wake expansion.

Blackmore et al [4] used experiments to investigate the effects of turulence on the drag of solid discs and porous disc turbine simulators.

Aubrun et al (2013) [2] studied wind turbine wake properties, by comparing a non-rotating simplified WT, based on the AD concept, and a rotating model, to determine the limits of the simplified model to reproduce a realistic wake. Concluding that the wakes, in the modeled ABL, were indistinguishable after 3D downstream. (in relatively high turbulent inflow conditions. Discrepancies still exist at x/d = 3 in low turbulent inflow conditions, but are relatively minor. So the simplified AD model seems to be usable to reproduce the far wake.

2.0.2 Use in CFD simulations

Numerical simulations and experimental studies can compliment each other for a better understanding.

As mentioned, wind turbines are large, on the order of hundreds of meters, with a typical spacing within a farm of 5-10 D, and a thickness of the blade on the order of 1m. In order to resolve the full turbine geometry, ideally one would need to build a mesh with submilimeter resolution in the blade BL inside a kilometer-scale computational box within the entire farm fits. As a consequence, we use a simplification: a model with an accuracy that generates the correct velocity deficit and TI in the far wake while ensuring that it is not too computanionally demaning. Thus, most codes rely on AD. [11] [8] [7] Such models are an attractive alternative, as they require fewer grid cells and not as small grid dimensions, allowing larger time steps. This efficiency comes at the expense of resolving the fine details of the blade BL, but if the objective is the far wake, this trade off is reasonable and AD is more than acceptable. As with experiments, a porous disc with the same diameter that applies a similar thrust force upon the moving fluid as a set of rotating blades may

be used, but turbulence structures shed from the disk vary compared to the rotor in the near wake. Thus, AD is well suited for full wind farm computations. And work is being done in developing these models and comparing them to experimental results [7] [11], including a organized workshop to compare different state-of-the-art numerical models for the simulation of wind turbine wakes [8], especially comparing wakes produced from simulations to those produced with experiments.

Also on the computational area, more work related to AD is needed. For example, [11] claims the need for implementing a model for the wind turbine towel and nacelle to assess their impact on the turbine performance and wake profile.

Obtaining both real and experimental data is necessary in order to develop simulation methods and check simulated observations and predictions against actual wake characteristics. Experiments also provide data for computational model validation and for comparison for future work.

However, with such further development, a relatively inexpensive tool for assesment of flowfields and planning of wind farms would be at hand for the industry (to enable the industrial use of CFD), and the CFD AD could be an accurate and validated method for numerically modelling turbines [16] [7].

2.0.3 Developing the actuator disk

One main issue remains, as there is no standard for designing and making the experimental actuator discs. Bossuyt et al (2016) [5] used a symmetric design, with a solidity that decreases with radial direction. Lignarolo et al (2016) [10] used a layered fine metal mesh, considered as a grid turbulence generator, while Aubrun et al [2] used fine metal meshes with varying porosity at the center of the disc and at the outer edge. Blackmore et al (2013) [4] used a hole pattern to maintain approximately uniform porosity across the radius. Aubrun et al [1] used both a metallic mesh with uniform porosity and a porous disc of plywood with radially non-uniform porosity. Sforza et al (1981) [16] used perforated metal plates, while Pierella and Sætran [15] used wooden grids. Myers et al (2010) [13] used PVC plastic for their discs. Even though the simulated turbine will vary, and thus the diameter, porosity and drag coefficient of the disc, a standard design creating the desired wake would be practical to create uniformity and comparability between experiments, and to save time so that every researcher around the world does not need to start the phase by developing their own disk.

Neunaber [14] cut her disk from an aluminium plate in a non-uniform matter. She also highlited that she had a 100% blockage in the center, where the nacelle is located in the case of a turbine, and that blackage shoul vary linearly similar to a real turbine.

Another detail to take into consideration at this point is the wind-tunnel blockage efffects created by the turbine models which may affect the wake. Thus, it is desired for the discs to be small [16].

Also wanted further work, as to explain why a smaller diameter porous disc resulted in lower drag coeff than the larger diameter disc with same porosity. [4]

Nevertheless, in a direct experimental comparison of turbulent flow in the near wake, a porous disk (with same dimention and axial force as a rotating turbine) is currently not available [10]. Main drivers are porosity, structural stiffness, wake-flow uniformity

Chapter 3

Method

In the following, the process of designing and creating the Actuaor disk (AD) and measuring the drag in the wind tunnel will be explained, as well as the experimental setup.

3.1 Experimental setup

In order to measure the drag on the Wind turbine model (WTM) and the ADs, a wind tunnel and a force plate is needed as part of the experimental setup. There was also the need to construct a rig on which the turbines could be placed inside the wind tunnel.

3.1.1 Force plate, wind tunnel and associated equipment

The wind tunnel used is one meter wide and a half meter tall. It has a maximum velocity of 35 m/s and a turbulence intensity of ... Equipment can be placed inside the wind tunnel by removing a glass window which is 75 cm wide and 35 cm tall. The wind velocity is changed by manually turning a wheel, that in turn changes the position of the valves next to the motor inside the tunnel, hence changing the velocity. In the floor of the tunnel there is a small hole, making it possible to connect the item one is measuring forces on inside the tunnel to the load cell underneath the tunnel.

Underneath the wind tunnel is a force plate of the type AMTI BP400600HF 1000, able to measure the force and moments components along the x-, y- and z-axes. Here, the x-axis is defined to be along the length of the wind tunnel, parallelly to the wind velocity. The y-axis is defined to go across the width of the tunnel, while the z-axis goes along the height of the tunnel. Further, the origin is defined to be at the tunnel floor, in the center of the tunnel, as seen in figure **??**. The force plate can measure forces as low as ... and has an accuracy of ...

The drag measured on the load cell is sent as a voltage signal through an amplifier. After-

wards, it is sent through a low pass filter, with a cut-off frequency of 1000 Hz. The data was gathered and saved using LabView, and the signal was turned back into a force using the given relationship between voltage and newton.

Inside the tunnel there is a sensor measuring the temperature, and a pitot tube measuring the pressure. The signal from the pitot tube is also saved as a voltage, which is later used to quantify the wind velocity.

A potential uncertainty related to the wind tunnel is the fact that the pitot tube is placed in the center of the tunnel, at y=0, z=0.25 m, $x \approx -4m$. Thus, the velocity measured is not necessarily the same as the velocity that hits the WTMs, which are placed close to the floor of the tunnel. Due to the development of wall boundary layers, the velocity hitting the WTMs is likely lower than the measured and registered velocity.

3.1.2 The rig

The test rig consisted of a magnetic steel bar of 0.5 m stretching across the width of the wind tunnel, on top of a aluminum cylinder which connects the bar to an aluminum plate, that in turn can be strapped to the load cell underneath the wind tunnel. The bar was lifted about a centimeter above the ground floor of the wind tunnel.

Initially, it was desired to have the steel bar be almost as long as the width of the wind tunnel, in order to avoid affecting the flow outside of what is already the boundary layer in the tunnel. Similarly, it was desired to have the hub of the turbines exactly in the vertical middle of the tunnel, at z=0.25 m, to avoid the boundary layers. However, this was not doable. The hole in the bottom of the wind tunnel was limited in size, which meant that the steel bar could only be connected to the load cell underneath the tunnel through one aluminum cylinder with a small diameter of about 2 cm, making the support less robust. The length of the metal bar had to be shortened, and the bar had to be brought closer to the tunnel floor, in order to avoid bending and flapping at the ends.

3.2 Wind turbine models

The two-bladed rotating WTMs are the property of KTH in Stockholm. They have a diameter of 45 mm, and a hub height of approximately 65 mm. Magnets are incorporated into the bottom of the models.

3.3 The actuator disks

As mentioned, there are no standard way of designing actuator disks. It was desirable to create ADs with multiple solidities, and a possible method that suggested was to create two ADs that are connected and can be rotated relative to each other, in order to change the solidity. However, this seemed hard to achieve at such small scales as are relevant in this work. In addition, the author was skeptic to the method based on the results of [15], showing that a monoplane and a biplane AD made with the same shape and porosity

produced different drags, making the cases not comparable. Since making a monoplane disk is perhaps simpler and easier to recreate, this method was preferred.

3.3.1 Computer-aided design and 3D printing

The actuator disks, as well as their stands, were designed using SolidWorks. Cura was used to turn the designs into readable code for the 3D printers, and the parts were then printed using a printer of the type Ultimaker 2+. The material used was PLA.

A significant limitation occurred during the design process. The 3D printers available could not print thinner than 0.4 mm, meaning that each line in the disks had to be at least 0.4 mm. However, printing lines of 0.4 mm proved troublesome, and it was decided that all lines should be equal to or thicker than 0.5 mm. This is a significant size given that the disks are in themselves of such small dimensions. So it turned out to be a limit to how porous the disks can be made.

In general, a concern when using 3D printers is the fact that the print is not a hundred percent equal to the design - small variations may occur, making the actuator disks with the same design slightly different from each other. These slight variations matter more when the overall size of the design is so small compared to a larger design, however, the variations are still so few and small that they are considered to have close to no effect on the solidity or in making the disks differ from each other. In comparison, other methods of making ADs may also lead to minor differences.

3.3.2 Design of the tower

The tower was designed to have the exact same dimensions as the given wind turbine model's tower. Most importantly, it had a hub height of 65 mm. Underneath there was made a hole that could fit a cylindrical neodymium magnet with a diameter of 10 mm, a height of 2.5 mm and a strength of 0.9 kg. The actuator disks were made to be interchangeable, and thus the end of the tower where the actuator disks will be connected is made slightly thinner in order to fit into the designated holes in the actuator disks. Three towers were printed.

3.3.3 Actuator disk design

The actuator disks were designed with a diameter of 45 mm, to match the wind turbine models. The thickness of the disks is 2.5 mm.

Two different designs of actuator disks have been tested. The first has numerous equally-sized holes spread symmetrically around the center point of the disk. This design is meant to be similar to those actuator disk designs made by a thin metal grid, comparable to a grid turbulence generator. The second design is also symmetric around the center point, but this one has rectangular (however filled in to avoid sharp corners) holes that vary in size with radial distance, increasing in size as the radial coordinate increases. Thus, the solidity decreases with radial coordinate, matching the characteristics of an actual WT.

For each of these configurations, two degrees of solidity was used as an initial try. The chosen values were 60% and 40%. A solid disk was also made and tested as a reference case. Three disks of each design and solidity were printed.

Each disk was as mentioned made with a small hole in the center, used to connect the stand to the disks. Thus, this hole was filled in during the tests in the wind tunnel, and did not affect the solidity. This resulted in a larger solidity in the center of the disks, which can be argued to represent the nacelle of a WT.

Based on the resulting drag profiles from the initial round of testing, two sets of actuator disks with a solidity of 35% were designed and made. The first was made based on the design with equally sized holes. Due to the mentioned limitations regarding the printing thickness, there was a limit to how low the solidity could get, and providing a solidity less than 39% proved problematic. Hence the design was slightly changed, allowing for the holes to also cover the edges of the actuator disk. It was kept in mind that this results in a different disk circumference, and that this might result in a drag force unrelated to the previously tested disks. The second design was made as the designs with rectangular holes that vary in size with radial distance.

3.4 Testing

The rig was connected to the force plate using bolts, in such a way that the aluminum cylinder came up through the hole on the bottom of the tunnel. The rest of the hole was covered with tape. Careful consideration was taken when adding the tape, so that the aluminum cylinder did not touch anything, as that would affect the force measurements.

Given that the size of the wind turbine models is quite small, the turbines were tested in the wind tunnel three at a time, to ensure that the drag would be of an order that the instruments were able to measure and of an order where slight changes in the design resulting in slight changes in drag would be noticeable. The turbines were placed with a distance of 4D between them along the steel bar. The same was the case for the actuator disks.

Even though the turbine models were magnetic, it proved problematic to make them stay in the same position, with the turbine perpendicular to the wind direction, as the wind velocity increased. Thus, the models were connected to the steel bar using small pieces of tape. The 3D printed towers were able to stay in the right position on the base by themselves, still they were taped to the base like the rotating turbine models, to make sure the cases were comparable.

As the drag is the force of interest in this work, only the force in the x-direction is measured. The force was measured for five different wind velocities; 5 m/s, 7.5 m/s, 10 m/s, 12.5 m/s and 15 m/s. This corresponds to Reynolds numbers all of the order 10^4. Since the velocity was changed by manually turning a wheel, a slight difference in the velocities occurred between the different measurements.

The force plate drifted over time, as is often the case with force measuring equipment. To take this into consideration when measuring the forces, zero measurements were conducted before and after every measurement. A 20 second tare measurement was first con-

ducted. The wind tunnel was then turned on, with the velocity initially set to about 1 m/s, and then turned up to the desired value. A measurement lasting 60 seconds was then conducted. The velocity was once again reduced to about 1 m/s, and the wind tunnel was shut off. After the wind tunnel had quiet down and there was close to no moving air inside, another 20 second tare measurement was conducted. When measuring, a sampling rate of 1000 samples per second was used.

Besides measuring the drag on the rotating turbine models and on all the different sets of actuator disks, a measurement was also conducted measuring only the drag on the base and the towers, without having any disks connected to them.

3.5 Calculations

For each disk at each wind velocity, the data collected from the wind tunnel consisted of a time series of voltages corresponding to the measured force and the measured wind velocity, as well as the times for when the first zero measurement and the second zero measurement were conducted and when the 60 second measurement started. Using Matlab, this data was treated.

A linear drift of the force plate was assumed. Thus, using the two zero measurement values, a linear function approximating the drift was created. The part of this linear function corresponding to the 60 seconds where the force measurement was conducted, was extracted. For each measured force in the time series, the corresponding drift was subtracted. After, the average force over the time series was calculated, as well as the variance and standard deviation.

In the same matter, the drift was subtracted and the average force was calculated for the measurements of only the base and the tower. This was done for each of the different wind velocities. These averages were then subtracted from the averages calculated earlier, so that the final drag force represented only the force on the disks, excluding the towers and the base.

Finally, this calculated drag was divided by three, so as to only consider the drag on one disk. This force was used in calculating the drag coefficient, together with the total swiping area of the rotating turbine model, being πr^2.

Another value collected from the measurements was the average temperature during the 60 seconds of measuring, used to decide on the appropriate value for the air density when calculating the drag coefficient.

Chapter 4

Results & Discussion

After conducting the measurements, profiles showing the drag coefficient as a function of the wind velocity could be created for each set of disks, as well as for the rotating WT models. In this section, the drag and drag coefficient profiles are presented and discussed, as well as the calculated average Cd and the standard deviations. In the end, the measurement noise is discussed.

4.1 Rotational WT model

The first measurement conducted using three rotating WT models resulted in a drag coefficient that was relatively independent of wind velocity for four of the measured wind velocities, but with a significant deviation at 5 m/s. To investigate whether this deviation was due to a measurement error, a second measurement was conducted, this time using three new rotating WT models. This second measurement gave more of an expected result at 5 m/s, however showed a deviation at 15 m/s. Thus, a third measurement, once again with three new rotating WT models, was conducted. Finally, a fourth measurement was carried out, this time using the same models as during the third measurement. The resulting drag coefficients can be seen as a function of wind velocity in figure 4.1.

As can be seen, there is some variation between the different measurements. The values from the third and the fourth measurement, conducted using the same WT models, are quite similar at 5 m/s, 7.5 m/s and 12 m/s, and at 15 m/s, they completely overlap. This may show that the measurement is repeatable, and that one of the reasons for the varying results is simply that the rotating WT models have small differences, for example related to the friction of the rotating blades and how well they are connected. Be it too tight, there will be added friction. Be it too loose, the blades may start to oscillate. However, even between the third and fourth measurement, there is a noticeable difference at 7.5 m/s, showing that differences between the WT models is not the only cause for the varying results.

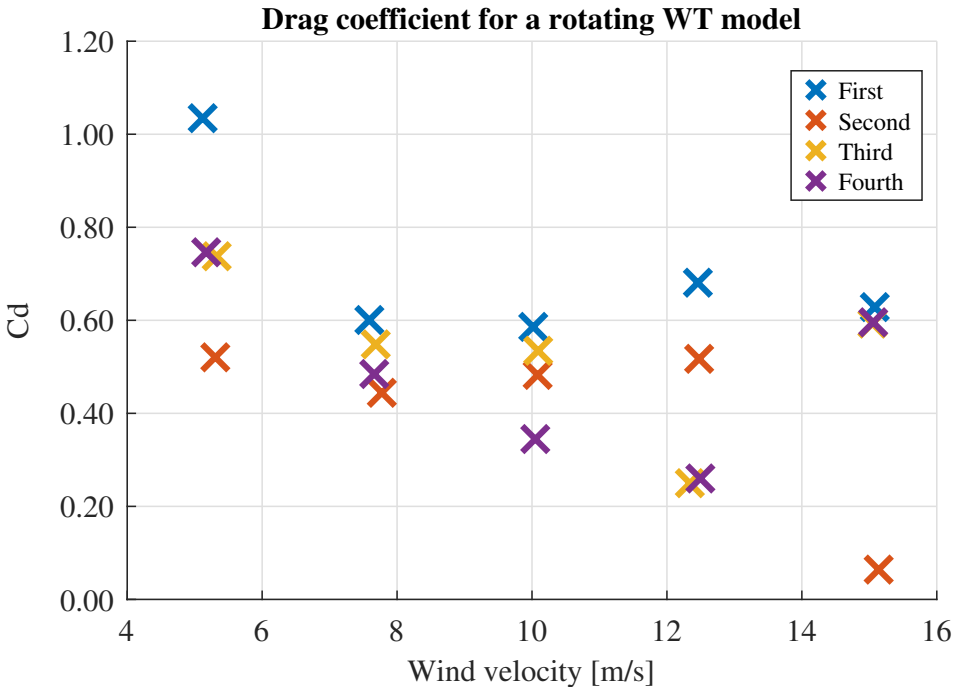

Figure 4.1: The drag coefficient for the rotating WT models, obtained through four rounds of measurements.

Other possible causes of this variation may be related to noise and fluctuations in the applied wind velocity and in the force plate.

To investigate the results further, the drag resulting from the different measurements are pictured as a function of wind velocity in figure 4.2

The drag at 12.5 m/s is lower than the drag at 10 m/s for the third measurement set, and the drag at 15 m/s is lower than the drag for 12.5 m/s for the second measurement set. This is not physical, and thus it is assumed that these two values are errors. The drag measured during the fourth measurement coincides with the disregarded drag from the third measurement, and is thus also regarded as an outlier. The wind tunnel did, for some unknown reason, seem to produce larger amounts of noise on the signal for velocities between 11 and 13 m/s, which might explain this repeated deviation. The drag at 10 m/s for the fourth measurement is higher than the drag at 7.5 m/s, however the value is lower than for all the measurements which seem to coincide quite well, and thus this value is considered as an outlier. The initial suspicious value, measured at 5 m/s in the first measurement, results in a C_d larger than one, which seems unlikely, and hence this value is also regarded as an outlier.

The outlier seem to be spread out both in terms of velocity at which they occur and in terms of whether they exceed or fall below the other values. One can argue that if taking a large

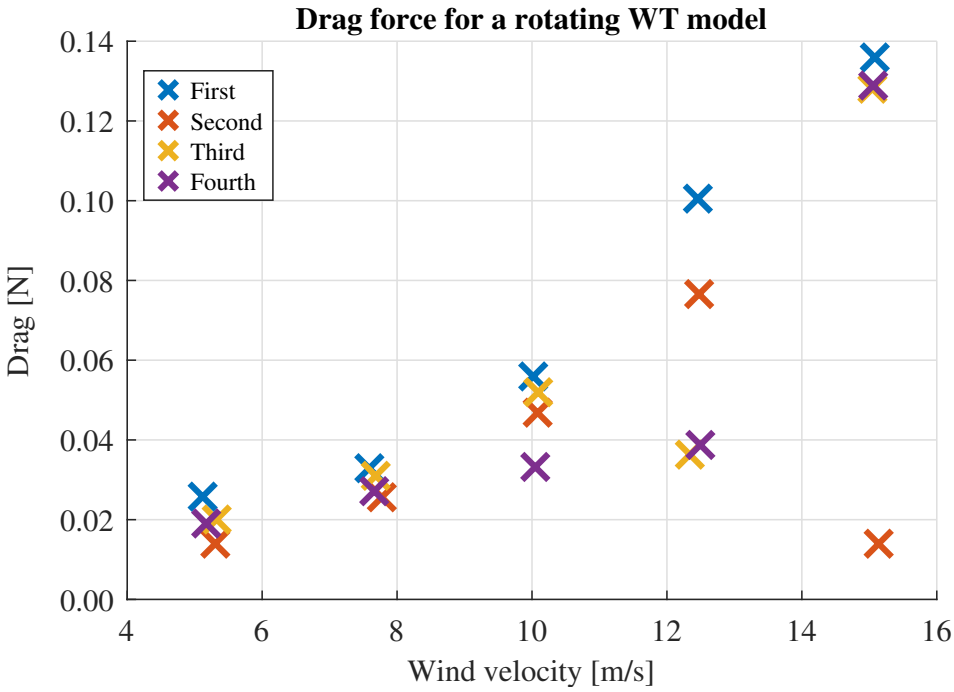

Figure 4.2: The measured drag for the rotating WT models, obtained through four rounds of measurements.

number of new measurements, they would have a Gaussian distribution about a mean, and that taking the average of the values that seemingly coincide would be representative for this total mean.

Thus, in order to achieve a representative value for the drag coefficient of the rotating WT models, the outliers were removed, and the average of the remaining drag coefficients was taken. This resulted in the drag coefficients seen in figure 4.3.

Assuming that C_d is Reynolds number independent for such a short span at Reynolds numbers, the average over these measurement points is taken, resulting in an average C_d of 0.585. Based on all the applied values, the standard deviation at hand is... Thus, when creating the ADs, this is the desired drag coefficient.

4.2 Drag on the ADs

The drag coefficient on the produced ADs has been studied. Initially, the solid disk, used as a reference case, produced the drag seen in figure 4.4a and the drag coefficient seen in figure 4.4b. Further, the drag and the drag coefficient for the two types of disks with 60% solidity can be seen in figure 4.5a and 4.5b, respectively. For all three disks, the drag is seen to increase with increasing wind velocity, as one would expect. The average drag

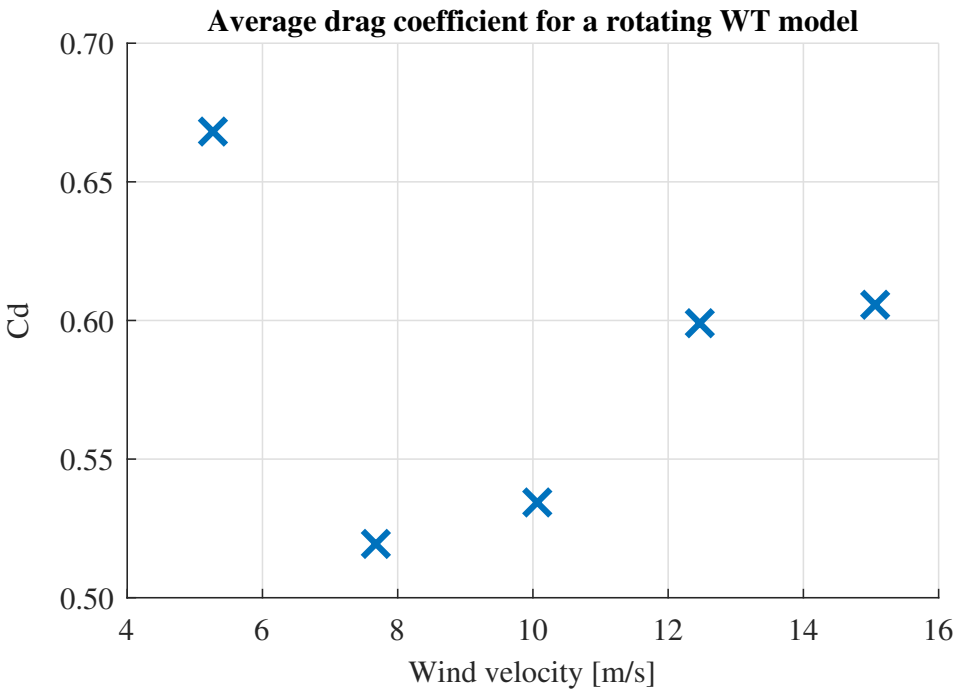

Figure 4.3: The average drag coefficient for the rotational WT models for each wind velocity, based on the four conducted measurements, after removing the assumed wrongful outliers.

coefficient and the standard deviation is presented in table 4.1.

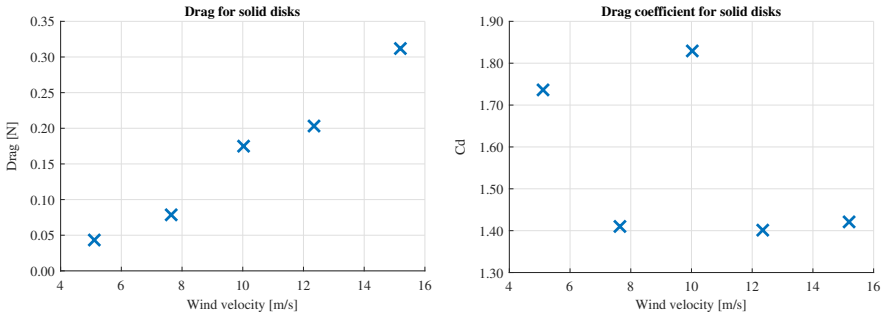

(a) The drag.

(b) The drag coefficient.

Figure 4.4: Using the solid disk.

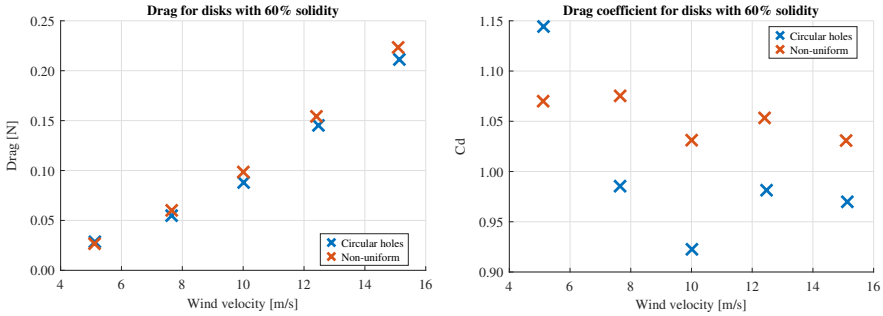

(a) The drag.

(b) The drag coefficient.

Figure 4.5: Using the disks with 60% solidity.

Further, the drag and drag coefficient for the disks with 40% and 35% solidity were plotted in figure 4.6 and 4.7. As these disks produced a drag coefficient fairly close to the average drag coefficient of the rotating turbines, this value is also included in the plots. The average drag coefficient and standard deviation can be seen in table 4.1.

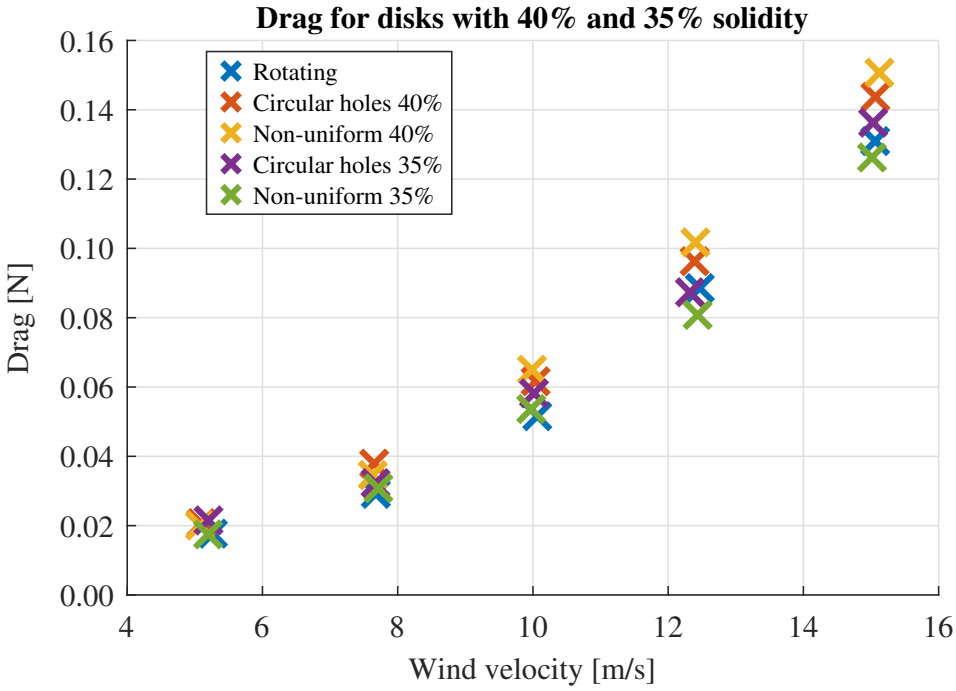

Figure 4.6: The drag for the disks with 40% and 35% solidity, compared to the average drag coefficient of the rotating disks.

Some general trends can be observed. For all disks presented in figure 4.7, as well as

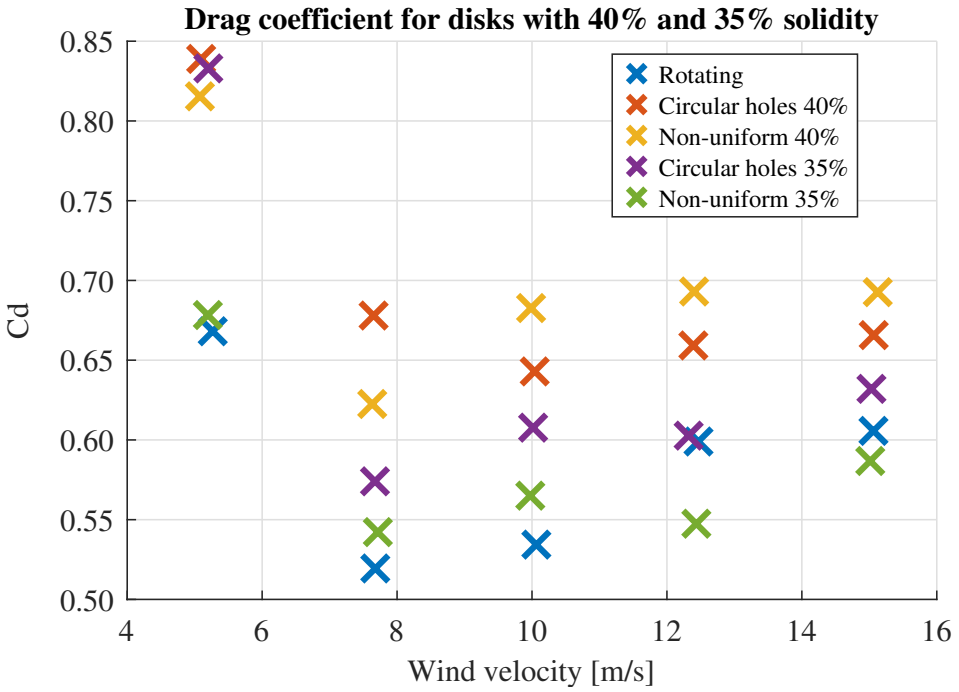

Figure 4.7: The drag coefficient for the disks with 40% and 35% solidity, compared to the average drag coefficient of the rotating disks.

for the disk with circular holes at 60% solidity in figure 4.5b, Cd measured at 5 m/s is significantly higher than for the other velocities, while the measurements at the four other velocities seem to concentrate around some mean value. This may be a result of ...

Disk type	Average Cd	SD
Rotating average	0.5853	
Solid	1.5596	
Uniform holes, 60%	1.0007	
Non-uniform, 60%	1.0521	
Uniform holes, 40%	0.6970	
Non-uniform, 40%	0.7013	
Uniform holes, 35%	0.6499	
Non-uniform, 35%	0.5840	

Table 4.1: Average Cd for each disk.

In terms of these results, the non-uniform disk can be seen to produce a slightly higher drag at the same solidity compared to the uniform disk at 60% and 40% solidity. The same trend can not be seen at 35% solidity, however this design with holes is created in

a different way, with a larger circumference, and may not be exactly comparable. The non-uniform 35% disk seems to best match the rotating WT model.

As can readily be seen, the drag coefficient decreases with decreasing solidity, as one would expect. This can be compared to [10], who presented a comparison between different drag coefficients as a function of solidity as presented in six different studies found in literature. According to this, a solidity of 60% results in a Cd of around 0.9, a solidity of 40% results in a Cd between 0.5 and 0.6, and a 35% solidity results in a Cd between 0.4 and 0.5. Compared, the disks used in this study presents a higher drag for all solidities. This can be caused by conditions such as inflow turbulence.

4.3 Noise and other possible sources of error

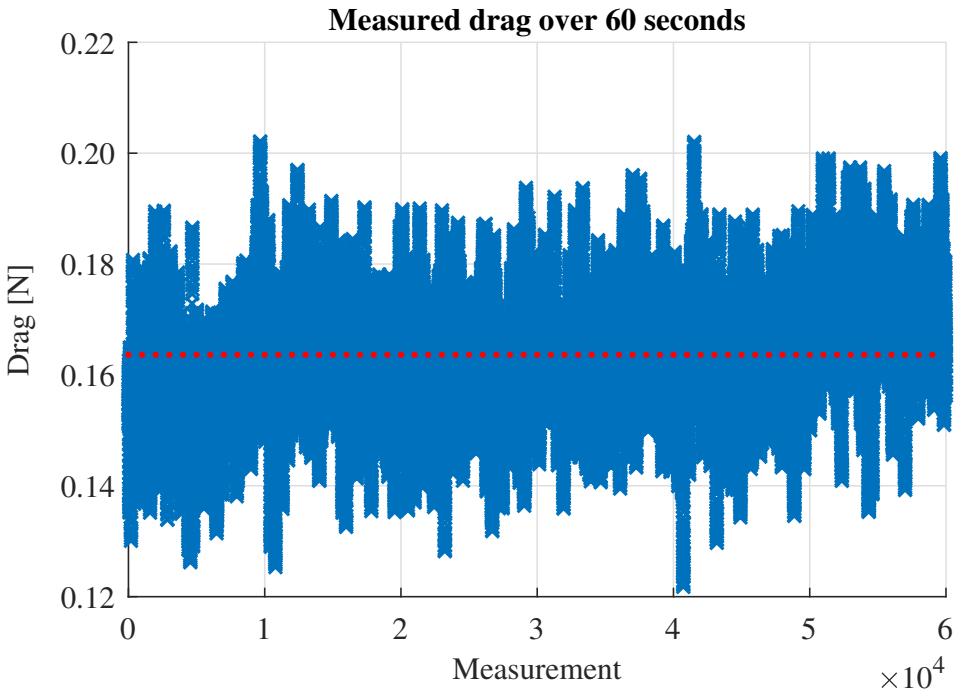

Figure 4.8: The drag for the solid disk at 5 m/s.

Figure 4.8 shows each measured drag value at a sampling rate of 1000 Hz over the course of 60 seconds. The measured drag varies with a 0.012, compared to an average of 0.1636. This means that the noise is of one order less that the average.

This noise may both be related to measurement noise in the force plate, and electrical noise as the signal passes from the force plate, through the amplifier and the lowpass filter. It is still a reasonable assumption that the measurements have a Gaussian distribution and that the average drag is representative.

The measured temperature only varies between about 20°C and 23°C. Since this variation is fairly small, it is assumed to not have any significant impact on the resulting drag.

Chapter 5

Future work

As concluded in [], in order to create an AD matching a WTM, the wake must be similar. Matching the drag coefficient is only the first step in this process.

Going forth, the rotating disks and the ADs with the closest matching drag coefficient will be studied using Particle Image Velocimetry, both in front of and behind the models. This method can be used to, amongst others, study the velocity deficit and the turbulence intensity in the wake. It is also desired to integrate the wake in order to find the axial induction factor.

Further, the plan is to acquire 100-150 rotating WTMs, and set them up as a wind farm in a larger wind tunnel. The same thing will be done with the AD that most closely matched the drag and wake. This will be done in order to study the effect and suitability of using ADs when modelling large wind farms.

Chapter 6

Conclusion

Bibliography

[1] S. Aubrun, M. Bastankhah, R.B. Cal, B. Conan, R.J. Hearst, D. Hoek, M. Hölling, M. Huang, C Hur, B. Karlsen, I. Neunaber, M. Obligado, J. Peinke, M. Percin, L. Saetran, P Schito, B. Schliffke, D. Sims-Williams, O. Uzol, M.K. Vinnes, and A. Zasso. Round-robin tests of porous disc models. *Journal of Physics: Conference Series*, 1256:012004, jul 2019.

[2] S. Aubrun, S. Loyer, P. Hancock, and P. Hayden. Wind turbine wake properties: Comparison between a non-rotating simplified wind turbine model and a rotating model. *Journal of Wind Engineering and Industrial Aerodynamics*, 120:1–8, 09 2013.

[3] R. J. Barthelmie and L. E. Jensen. Evaluation of wind farm efficiency and wind turbine wakes at the nysted offshore wind farm. *Wind Energy*, 13, 04 2010.

[4] Tom Blackmore, William Batten, Gerald Muller, and AbuBakr Bahaj. Influence of turbulence on the drag of solid discs and turbine simulators in a water current. *Experiments in Fluids*, 55, 12 2013.

[5] Juliaan Bossuyt, Michael Howland, Charles Meneveau, and Johan Meyers. Measurement of unsteady loading and power output variability in a micro wind farm model in a wind tunnel. *Experiments in Fluids*, 58, 12 2016.

[6] S. Cannon, F. Champagne, and A. Glezer. Observations of large-scale structures in wakes behind axisymmetric bodies. *Experiments in Fluids*, 14:447–450, 05 1993.

[7] M.E. Harrison, William Batten, Luke Myers, and AbuBakr Bahaj. Comparison between cfd simulations and experiments for predicting the far wake of horizontal axis tidal turbines. *Renewable Power Generation, IET*, 4:613 – 627, 12 2010.

[8] Lorenzo Lignarolo, Dhruv Mehta, Richard Stevens, Ali Yilmaz, Gijs Kuik, Søren Andersen, Charles Meneveau, Carlos Ferreira, Daniele Ragni, Johan Meyers, Gerard van Bussel, and Jessica Holierhoek. Validation of four les and a vortex model against stereo-piv measurements in the near wake of an actuator disc and a wind turbine. *Renewable Energy*, 94:510–523, 08 2016.

[9] Lorenzo Lignarolo, Daniele Ragni, Carlos Ferreira, and Gerard van Bussel. Kinetic energy entrainment in wind turbine and actuator disc wakes: An experimental analysis. *Journal of Physics: Conference Series*, 524:012163, 06 2014.

[10] Lorenzo Lignarolo, Daniele Ragni, Carlos Ferreira, and Gerard van Bussel. Experimental comparison of a wind-turbine and of an actuator-disc near wake. *Journal of Renewable and Sustainable Energy*, 8:023301, 03 2016.

[11] Luis Martínez Tossas, Matthew Churchfield, and Stefano Leonardi. Large eddy simulations of the flow past wind turbines: actuator line and disk modeling: Les of the flow past wind turbines: actuator line and disk modeling. *Wind Energy*, 18, 04 2014.

[12] Johan Meyers and Charles Meneveau. Optimal turbine spacing in fully developed wind farm boundary layers. *Wind Energy*, 15:305 – 317, 03 2012.

[13] Luke Myers and AbuBakr Bahaj. Experimental analysis of the flow field around horizontal axis tidal turbines by use of scale mesh disk rotor simulators. *Ocean Engineering*, 37:218–227, 02 2010.

[14] Ingrid Neunaber. *Stochastic investigation of the evolutoon of small-scale turbulence in the wake of a wind turbine exposed to diffeent inflow conditions*. PhD thesis, Carl von Ossietzky Universitat Oldenburg, 11 2018.

[15] Fabio Pierella and Lars Sætran. Effect of initial conditions on flow past grids of finite extension. *17th Australasian Fluid Mechanics Conference 2010*, 01 2010.

[16] P. Sforza, P. Sheerin, and M. Smorto. Three-dimensional wakes of simulated wind turbines. *Aiaa Journal - AIAA J*, 19:1101–1107, 09 1981.

List of Acronyms

AD Actuaor disk. 11

WTM Wind turbine model. 11, 12